ACS SENSORS

pubs.acs.org/acssensors

Article

Smartphone-Integrated Label-Free Rapid Screening of Anemia from the Pattern Formed by One Drop of Blood on a Wet Paper Strip

Sampad Laha, Aditya Bandopadhyay, and Suman Chakraborty*

Cite This: *ACS Sens.* 2022, 7, 2028−2036

Read Online

ACCESS | Metrics & More | Article Recommendations | Supporting Information

ABSTRACT: Screening of anemic patients poses demanding challenges in extreme point-of-care settings where the gold standard diagnostic technologies are not pragmatic and the alternative point-of-care technologies suffer from compromised accuracy, prohibitive cost, process complexity, or reagent stability issues. As a disruption to this paradigm, here, we report the development of a smartphone-based sensor for rapid screening of anemic patients by exploiting the patterns formed by a spreading drop of blood on a wet paper strip wherein blood attempts to displace a more viscous fluid, on the porous matrix of a paper, leading to "finger-like" projections at the interface. We analyze the topological features of the pattern via smartphone-enabled image analytics and map the same with the relative occupancy of the red blood cells in the blood sample, allowing for label-free screening and classification of blood samples corresponding to moderate to severe anemic conditions. The accuracy of detection is verified by comparing with gold standard reports of hematology analyzer, showing a strong correlation coefficient (R^2) of 0.975. This technique is likely to provide a crucial decision-making tool that obviates delicate reagents and skilled technicians for supreme functionality in resource-limited settings.

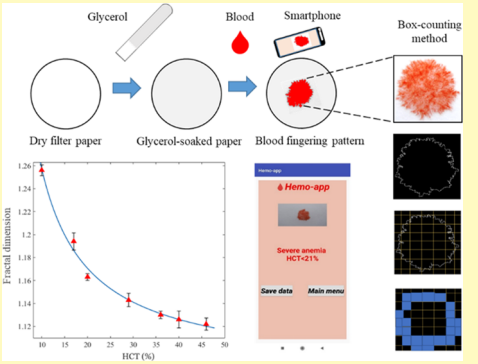

KEYWORDS: *anemia screening, hematocrit, paper-based biosensor, fractal dimension, box-counting method, extreme point-of-care diagnostics*

Anemia is a global public health challenge bearing major consequences in life, livelihood as well as socioeconomic development, especially pertaining to maternal and child health.[1] Hallmarked often by below threshold level of hemoglobin in the red blood cells (RBCs), anemia may stem from several possible reasons or combinations thereof, including insufficient RBC production, excessive destruction or loss of RBCs due to infections, and blood loss in women in their reproductive years or other hemorrhagic conditions. While nutritional deficiency (typically iron deficiency) appears to be a major factor behind anemia being prevalent in underserved communities,[2,3] other chronic[4] or acute diseases,[5] often undetected at early stages, may turn out to be of no less implications in dictating the underlying health conditions.

Being a public health challenge, anemia needs to be addressed via mission-oriented programs interfacing directly with communities and community workers, as well as other programmes targeting food security, water quality, hygiene, and infectious disease control. While securing the availability of food providing the essential nutrition remains critical in combating this challenge from an ecosystem perspective, extensive diagnostic testing appears to be the most imperative consideration that, going far beyond a restrictive subjective viewpoint of symptomatic clinical assessment, is likely to provide an appropriate quantitative index leading to enhanced objectivity in the clinical decision-making procedure. This envisaged quantitative index, in turn, is likely to be strongly correlated with the fractional occupancy of RBCs in the whole blood, commonly known as hematocrit (HCT). Based on the normal reference levels of men and women, previous clinical studies prescribed a threshold HCT value of 37%, below which the subject is considered to be affected by anemia.[6,7] Further, in case of severe anemia or internal hemorrhage, HCT levels may reduce drastically (<21%) and the patient might require urgent blood transfusion for survival.[8]

While standard pathological procedure of HCT determination, commonly necessitating centrifuges[9] and hematology analyzers,[10] is premised on established laboratory infrastructure and skilled technicians, disruptions to the said paradigm of testing appear imperative when the same is to be conducted by minimally trained frontline health workers outside controlled laboratory settings. Accordingly, in a point-of-care (POC) format, several miniaturized platforms have been introduced over the past few years. For instance, Lee et al. reported the use of direct current response for detection of blood HCT.[11] However, this method was associated with

Received: April 14, 2022
Accepted: June 28, 2022
Published: July 8, 2022

Downloaded via SUKHOTHAI THAMMATHIRAT OPEN UNIV on November 9, 2022 at 05:28:15 (UTC).
See https://pubs.acs.org/sharingguidelines for options on how to legitimately share published articles.

© 2022 American Chemical Society

https://doi.org/10.1021/acssensors.2c00806
ACS Sens. 2022, 7, 2028−2036

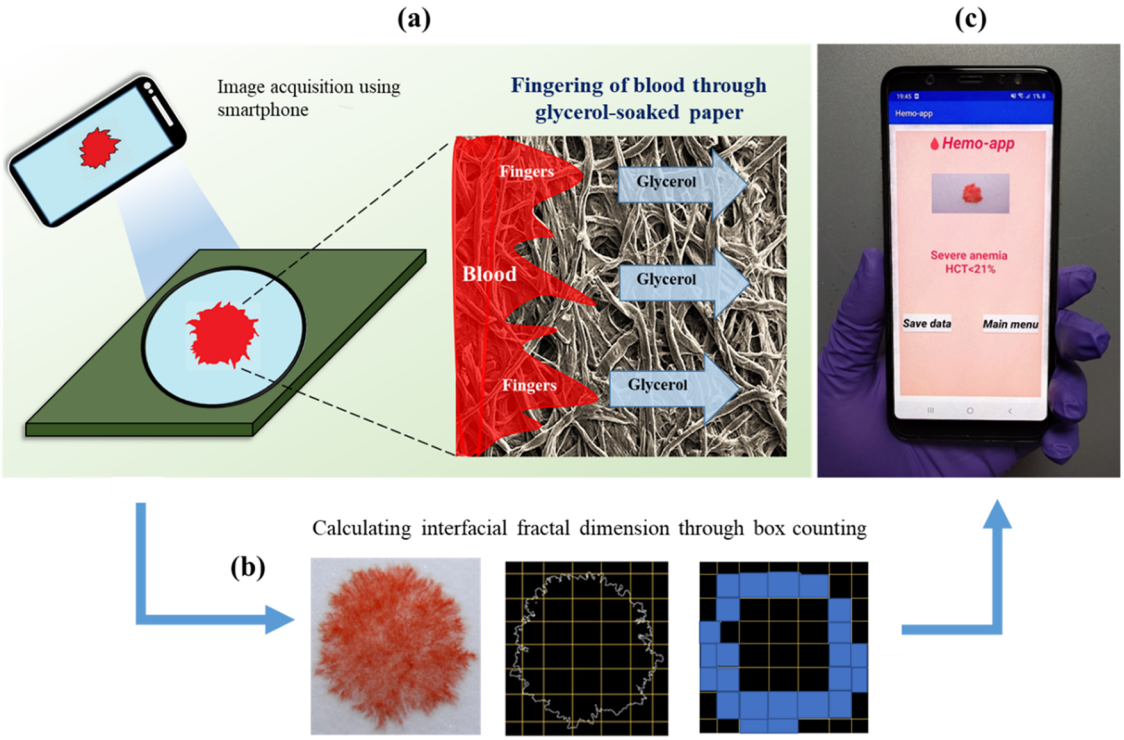

Figure 1. Schematic representation of the working principle of the anemia screening device. (a) Test setup that comprises a standard filter paper mounted on a back-strip and soaked in anhydrous glycerol. The blood (20 μL) is dispensed on the wet paper surface and the generated finger-like pattern is captured using a smartphone camera. The magnified view schematically shows how glycerol is being physically displaced across the paper pores by relatively less viscous blood, leading to the observed topology. The background of the magnified view is constructed via the scanning electron microscopic image (350X) of Whatman 1 filter paper for the realistic depiction of the physical phenomenon. (b) Captured image of the interface pattern being analyzed in a smartphone app, and the corresponding fractal dimension is determined based on the box-counting method. This fractal dimension maps with the HCT value of the blood sample, based on which the anemia screening is done. (c) Result-display screen of the in-house smartphone app (Hemo-app) showing the anemia screening result based on the HCT level, via suitable classification principles.

electrolysis bubbles, surfactant-induced hemolysis and RBC sedimentation that might destabilize the current signals and increase noise in output. Some optical methods of HCT measurement in microfluidic setup were also reported in the past few years, where the variation of greyscale intensity of blood may directly be mapped with the corresponding HCT value.[12,13] These methods, however, are strongly dependent on the ambient light intensity and may produce erroneous results with inevitable variations under the same under practical operating conditions. HCT detection has also been recently reported on a silicon chip using impedimetric techniques.[14] However, this approach of using RBC suspensions in phosphate-buffered saline instead of whole blood not only excludes the crucial effects of plasma conductivity that may compromise with the detection accuracy[15] but also renders it challenging for execution in POC settings. Centrifugal microfluidics was also utilized for HCT-level determination as well as complete blood counting applications on a plastic disk spun by a motorized unit.[16,17] Unfortunately, lack of uninterrupted power supply and nonbiodegradable waste disposal problems[18] have continued to pose a serious prohibiting limitation against the use of such centrifugal platforms in extreme POC settings.

Functionalized paper strips have of late emerged as viable platforms for rapid medical diagnostics from blood samples.[19−27] In a specific development concerning the estimation of HCT level on a paper microfluidic strip, Berry et al. developed a two-layered device that combined vertical and lateral channels engraved in the paper matrix to impose control on the cellular transport in the blood sample.[28] The fabricated layers were bonded by a double-sided permanent adhesive via patterning using a robotic cutting plotter. The color of RBCs was considered as a means to measure transport distances within the "thermometer"-like channel. Despite attempting for a simplistic approach, this method of estimation, however, was not designed to be quantitatively capable of being commensurate with the established laboratory standards. In addition, the act of paper device fabrication necessitated specialized manufacturing. Blood hemoglobin level estimation is another fundamental approach to assess anemia, and different miniaturized platforms including paper-based devices have been introduced accordingly.[29,30] For instance, Biswas et al. have recently developed a smartphone-integrated hemoglobin sensor in which detection is carried out based on colorimetric signals developed on a paper strip.[31] While this device offers accurate predictions at significantly low costs, it involves rigorous sample preparation and reagent dispensing steps where precise stoichiometric ratios need to be maintained to get reliable results. Moreover, such colorimetric detection systems may require proper refrigeration facilities for storing chemical reagents, which often becomes a big ask in resource-poor settings with unpredictable power supply and inadequate infrastructure. Of late, Frantz et al. have reported a smartphone-enabled technique of HCT determination by tracking the blood flow on a nonreaction lateral flow device.[32] This method is evidently rapid and cost-effective, but mandatorily necessitates high-resolution wicking videography that may not be trivial to implement at under-resourced sites

https://doi.org/10.1021/acssensors.2c00806
ACS Sens. 2022, 7, 2028−2036

by unskilled personnel. Furthermore, the lateral flow strip itself requires a specialized fabrication via collage of different types of specialized porous membranes.

From a critical review of the reported POC technologies on HCT determination or screening of anemia, certain compelling challenges appear to be evident, stemming from any of the following or combinations thereof: (i) requirement of sophisticated fabrication procedure of the diagnostic strips, (ii) requirement of sensitive reagents that either do not have an established supply chain at decentralized locations or may malfunction unless stored in stringently controlled refrigerated spaces, and (iii) specialized detection technology that may not work at extreme POC settings. Circumventing all of these constraints simultaneously, here, we report the development of a low-cost sensor for HCT level determination on a paper strip (for a schematic depiction of the methodology workflow, see Figure 1), by harnessing smartphone-enabled image analytics of the spontaneous spreading of one drop of finger-pricked blood on a wet paper strip. The fundamental premise of our detection methodology, as opposed to the traditional biochemical or bioelectrochemical route, is based on a completely physical principle of formation of finger-like interfacial patterns when a less viscous fluid displaces a more viscous one.[33−36] The resulting viscous fingering, popularly referred to as Saffman−Taylor instability,[34] has been a topic of interest in fluid dynamics research over the years, and the same remains to be poorly understood for complex fluids like blood. In the paper strip biosensor developed by us, we have attempted to uncover intriguing and hitherto-unaddressed facets of the latter and establish the same as a signature of the blood HCT level as blood sample spreads spontaneously in a glycerol-soaked paper. Recognizing considerable variation of this pattern for different HCT values, we further compute Hausdorff fractal dimensions (HFD) from the pixelated image and establish an exclusive mapping of the same with the blood HCT.

As opposed to any videography-based approach, the principle herein demands only one snapshot of the interfacial topology of the blood fingering pattern via a smartphone camera and performs quantifiable analytics solely based on it. As unique value-added propositions, off-the-shelf filter papers may be directly used for this detection without necessitating any subsequent fabrication steps. Other than soaking the paper with a stable and standard liquid such as glycerol that may even be available via a common consumer-based supply chain without any environmental-sensitivity concerns, there is no specialized reagent needed for the procedure. The detection may be completed as rapidly as within a span of about 30 s and the only job of the testing personnel is to capture a static image in a smartphone post dispensing the blood drop on the paper strip when alarmed via a smartphone-integrated automated signal. Other than the power required for regular smartphone charging, no electrical or other forms of power is required to run this test. Via disseminating this test at extreme under-resourced locations by unskilled personnel, this technology is demonstrated to be commensurate with results from gold standard laboratory-based procedures for extremely accurate classification of vulnerable patient groups suffering from moderate to severe anemic conditions, thereby addressing an outstanding global challenge targeted toward underserved community care.

EXPERIMENTAL SECTION

Sample Collection and Study Approval. Human whole blood samples were collected from the pathology laboratory of B. C. Roy Technology Hospital, Indian Institute of Technology Kharagpur, after obtaining the requisite approval of ethical clearance from the Institute Ethical Committee (IEC No. IIT/SRIC/DR/2017). We performed all our experiments with freshly drawn blood samples collected in ethylenediaminetetraacetic acid (EDTA) tubes. A total of 70 different blood samples were analyzed for establishing the detection procedure. Due to nonavailability of blood samples of ultralow HCT levels directly drawn from the participating human subjects, blood samples of HCT values ranging from 10 to 20% were prepared by diluting higher HCT samples with isotonic saline solution. Each experimental run was executed with only 20 μL of blood sample. All of the experiments were conducted within 30 min of drawing the blood to avoid any structural and functional damage of RBCs due to prolonged storage (greater than 4 h) in EDTA.[37] We conducted some experiments with blood stored in EDTA tubes for different durations of time, to find the extent of errors introduced while using stored blood (for more details, refer to Table S1). Aqueous solution (0.1% w/v) of Rhodamine B dye (Sigma-Aldrich) was used for carrying out control experiments on glycerol-soaked paper, in an effort to bring out the exclusive pattern formation characteristics intrinsic to human blood samples.

Substrate Preparation and Blood Dispensing. For illustration, we directly used Whatman 1 filter paper (diameter: 110 mm, average pore size: 11 μm) as the detection strip, without any further structural modification. The filter paper was soaked in anhydrous glycerol (Sigma-Aldrich) for 5 min and thereafter placed on a stable base to act as the test cartridge. Only 1 mL of anhydrous glycerol turned out to be sufficient to saturate each paper strip (having an area of 9503.3 mm^2). Anhydrous glycerol was chosen for its substantially higher viscosity compared to whole blood, transparency, biocompatibility, and ease of availability via an established supply chain without any storage concerns. Blood drops were dispensed from a height of ∼1 cm of the test strip to prevent splashing accompanied by unwarranted inertia-mediated effects (refer to Table S2 for more details). Within the permissible range of drop dispensing height, the observed angle made by the trajectory of the blood sample before reaching the paper strip as modulated by altering the angles of pipette tips in the control experiments, did not show any influence on the final test outcome. To ensure that the testing personnel do not dispense blood from a height beyond 1 cm from the paper surface, or, as a matter of fact—arbitrarily, a portable slider stage with a vertical height adjustment feature was provided as a modular handheld attachment along with the test strip. This attachment was simply placed adjacent to base cartridge for holding the blood dispenser. The height of the vertical slider can be adjusted in such a way that the blood droplet is assured to release from a suggested height (typically, 0.5 cm from the paper surface), irrespective of the degree of expertise of the user. To showcase the effect of ambient temperature on the detection performance, experiments were conducted in both inside and outside of the laboratory under different temperature conditions, the details of which have been provided in subsequent sections.

Detection Principle. The present detection principle delves on the exclusivity of the observed pattern of the spreading blood front in the pre-wet paper strip as against its HCT value. The fundamental scientific consideration dictating the above principle is premised on the phenomenon that when a less viscous fluid of viscosity μ_1 displaces a more viscous fluid of viscosity μ_2 in a porous medium, the interface between the two fluids may become unstable and exhibit finger-like patterns. The extent of this instability may be quantified by the log-mobility ratio, $R_m = -\ln\left(\frac{\mu_1}{\mu_2}\right)$,[33] as evidenced from the outcome of linear stability analysis for Newtonian fluids.[36] While the physical scenario addressed in this work is significantly more complicated because of the involvement of blood as a complex fluid as opposed to traditional Newtonian fluids, the essential physical principle may be quantified via a modified log-mobility ratio:

https://doi.org/10.1021/acssensors.2c00806
ACS Sens. 2022, 7, 2028−2036

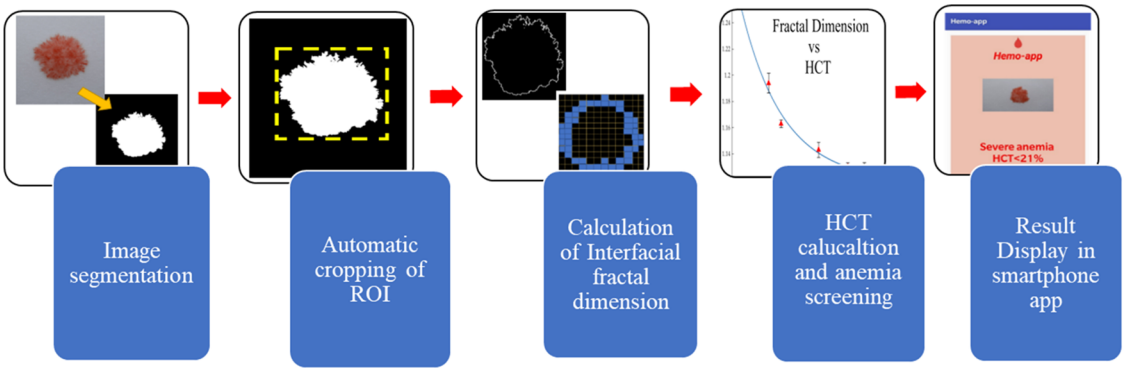

Figure 2. Flowchart showing the algorithm used for the extraction of hematological information from blood fingering pattern through a smartphone.

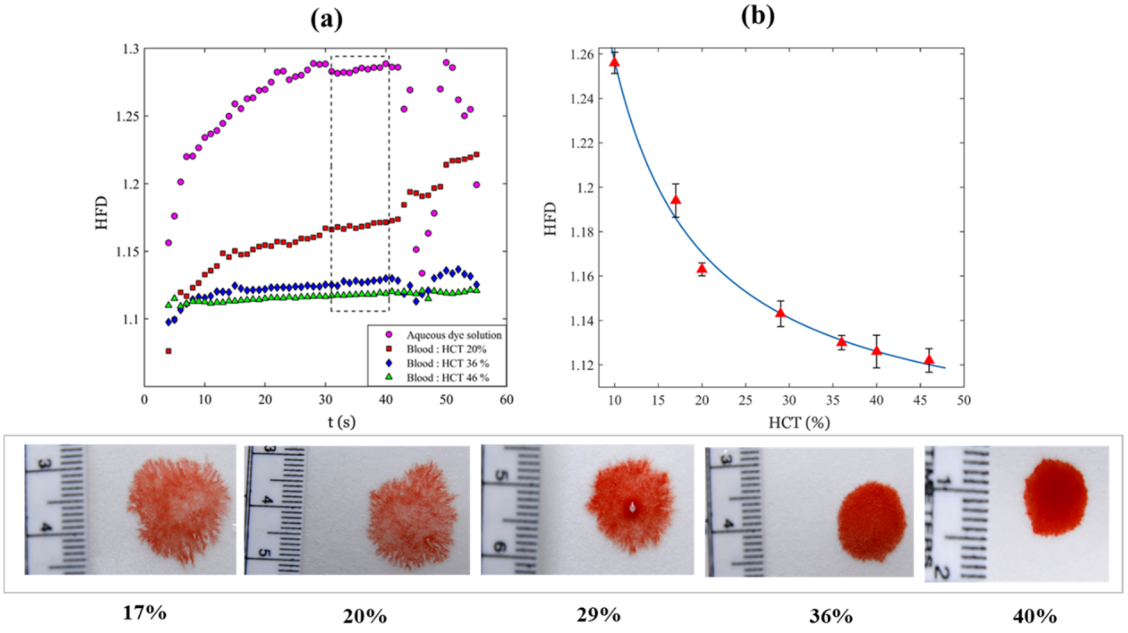

Figure 3. (a) Temporal variation of fractal dimension of patterns for the dye solution and blood of different HCT values. The rectangular box with dotted line indicates a stable time regime where the fractal dimension values are invariant. Beyond 40 s, random fluctuations in the fractal dimension value are observed as a result of mixing between the two fluids. (b) Variation of HFD of the blood interface (captured at 35 s) with HCT%, along with real-time experimental images of some representative scenarios (of varying HCT%), demonstrating the fingering phenomenon on a paper strip. It is seen that as HCT% increases, the interface complexity characterized by the corresponding HFD value decreases and vice versa.

$R_m = -\ln\left(\frac{\mu_{app}}{\mu_g}\right)$, where μ_{app} is the apparent viscosity of blood, which in turn is a function of its HCT value, and μ_g is the viscosity of anhydrous glycerol. Despite the inherent complexity of blood, its apparent viscosity may be reliably represented by a simplified power law model: $\mu_{app} = k\dot{\gamma}^{n-1}$,[38] where $\dot{\gamma}$ is the shear strain rate and the flow behavioral index n as well as the flow consistency index k are both functions of the blood HCT value.[38,39] From a collected compendium of human blood sample data via clinical research and organizing the same in a mathematically fitted framework,[38] the dependence of the parameters k and n on the blood HCT could be represented as: $k = C_1 e^{C_3 h}$, $n = 1 - C_3 h$, where h is the hematocrit expressed in fractional terms. Here C_1, C_2, and C_3 are constants virtually invariant to other conditions for a given animal species:[38] $C_1 = 0.0148\ P(s)^{n-1}$, $C_2 = 0.0512$, $C_3 = 0.00499$. By incorporating the above expression of apparent viscosity of blood, the modified log-mobility ratio could thus be expressed as

$$R_m = \ln\left(\frac{\mu_g}{C_1}\right) - (C_2 - C_3 \ln \dot{\gamma})h \quad (1)$$

Considering an average shear rate typical to standard testing conditions that remain virtually invariant under the capillary-driven pump-free spreading conditions of the blood samples as encountered in the testing practice (for details, refer to the Supporting Information), eq 1 can be expressed in the form $R_m = A - Bh$, where A and B are phenomenological constants, clearly establishing a linear decrease in the log-mobility ratio with increase in h over the domain of applicability of this equation (illustrated via practical data in Figure S1). Beyond a threshold value of h, R_m reduces to an extent that the finger-like structure at the blood−glycerol interface tends to disappear altogether. Physically, this may be attributed to a statistically more uniform blockage of the otherwise random pores in the fibrous paper matrix by RBCs that leads to a stable, virtually uniform liquid front when the blood sample has relatively high fractional occupancy of the RBCs. The effective viscosity of such high-HCT blood samples appears to be beyond a threshold limit to trigger substantially enhanced diffusive transport of momentum across the interface in a

https://doi.org/10.1021/acssensors.2c00806
ACS Sens. 2022, 7, 2028−2036

way to smear out the effect of the shear gradient between the blood and the glycerol. This, in turn, stabilizes the interface against the driving capillary forcing. The substrate porosity, thus, plays a crucial role in modulating the viscous fingering of blood on the paper strip, via explicit alteration in the shear rates, as evidenced from the data provided in the Supporting Information (refer to Figure S1).

Pattern Analysis and App Development. The first step in our analysis post obtaining the smartphone image of a spreading front of blood on the wet paper strip was to convert the RGB images of blood patterns to grayscale. Then, the blood pattern was segmented from the background using the Otsu thresholding method.[40] Next, the external contour of the blood pattern was determined, and using the contour information, a minimum area bounding rectangle was found out to crop the region of interest automatically. Thereafter, using the Canny Algorithm, the interfacial edge of the fingering pattern was determined. The extent of fingering of the pattern interface was quantified using the Hausdorff fractal dimension[41] (hereafter referred to as HFD or simply fractal dimension), which is a measure of the interfacial undulations. An in-house code based on box-counting method was developed to calculate the interfacial HFD of the fingering patterns[42] (for detailed steps of the box-counting algorithm, refer to Figure S2). A flow diagram of the image processing algorithm is presented in Figure 2.

We performed design optimization toward arriving at an optimal time window for the acquisition of one single static image of the fingering pattern. To accomplish this, we executed frame-by-frame analysis of the dynamically evolving topology of the blood−glycerol interface (explained in detail in the Results and Discussion section) and arrived at a time regime of 30−40 s (after the blood drop dispensing) over which the HFD value remained virtually invariant. Accordingly, a time alarm was arranged from the standard clock app available in all of the smartphones so that a static image could be automatically captured after 35 s from the dispensing of the blood drop on the paper strip.

In the tests demonstrated in this work, all of the images were captured using a Samsung Galaxy A6 Plus smartphone. By performing this imaging task using other smartphones as well, we could establish that the test results obtained out of our analytic procedure are effectively invariant of the specific smartphone camera, as attributable to the procedure of normalizing the image data. For executing all of the detection steps starting from image acquisition to analytics and result dissemination, a smartphone app (Hemo-app) was developed in-house. The application was written in Python 3.8.5 using Android Studio 4.0.1 and OpenCV 4.0.1 libraries. By training the detection algorithm with a large data set of blood pattern images, a functional relationship was established between the fractal dimension of blood pattern and the corresponding HCT value, which was subsequently classified for the screening of the severe and moderately anemic cases. Based on the derived fractal dimension value of the blood pattern, the Hemo-app categorizes the patient into any one of the three groups: severe anemia, moderate anemia, and normal.

RESULTS AND DISCUSSION

Determination of the Optimal Time Window for Imaging and Detection. The time evolution of the progress of the interface of the dispensed sample on the paper strip is depicted in Figure 3a. We observed that the complexity of the interfacial topology, characterized by the HFD value, initially increased with time and eventually saturated after ∼30 s due to the dominance of diffusion over advective spreading, as discussed earlier. Moreover, beyond ∼40 s, random fluctuations in the HFD values could be observed. Beyond 40 s, the interface appeared to be extremely diffused and blurred, precluding precise analytics.

The exclusive influence of blood as a complex fluid toward dictating the interface topology is also evident from Figure 3a, where the HFD values of the fingering patterns for the dye solution are perceptibly greater compared to that of the blood samples. This could be attributed to a significantly lower viscosity of water (dye solution) compared to the apparent viscosity of whole blood, resulting in an enhanced viscosity contrast with glycerol for the former case, leading to more discernible features of the fingering pattern. Further, the onset of the stabilized regime was observed to vary prominently with the HCT value of the blood sample, with early stabilization occurring for high HCT values. This could be attributed to a drastic attenuation of the viscosity contrast between blood and glycerol at high HCT values, resulting in a stabilization of the interfacial front.[39]

Test Performance and Validation. *Calibration Curve.* Figure 3b depicts the variation of fractal dimension of the blood patterns for different HCT levels. By least-square regression analysis (R^2 = 0.991), we obtained a statistically significant functional relationship (p-value = 0.0048) between the HFD of the interface patterns and the HCT value of blood (in percentage), which served as the standard calibration curve for the detection system

$$\mathrm{HFD} = (1.606 \times \mathrm{HCT}^{-0.9546}) + 1.079 \quad (2)$$

Repeatability analysis was verified using 10 different blood samples per HCT, each sample being repeated thrice. Figure S3 and Table S3 reflect the high reproducibility of the observed experimental trends.

Classification of Anemic Conditions. Based on the experimentally derived functional relationship between HCT % and HFD (as in eq 2), we identified two important threshold values of fractal dimension of the blood patterns, with respect to their pathological consequences. HFD values less than 1.130 indicate normal healthy condition, while those greater than 1.130 correspond to HCT < 37% and signify potential anemic concerns. Again, samples showing HFD values greater than 1.166 denote HCT levels below 21%, suggesting an urgent need of blood transfusion and/or other emergency life-saving measures.[8,43] Table S4 highlights the different classifications based on the threshold HFD values, having distinctive implications on anemia screening. Figure S4 outlines the sequence of operation of Hemo-app based on this principle, including on-screen declaration of the test outcome.

Validation Against Pathological Gold Standard. Figure 4 depicts the HCT levels as predicted by the present method for 74 whole blood samples as against the corresponding values obtained from an automated hematology analyzer deployed in gold standard pathology laboratory settings. This comparison revealed a high level of detection accuracy with a correlation coefficient (R^2) of 0.982. As shown in Figure 4, the black dashed line indicates the best linear fit for the derived HCT data, while the blue straight line indicates the 1:1 ideal case with a slope as unity. It is to be noted that the slope of the best fit line (1.0033) deviates only around 0.33% from the ideal scenario, thereby highlighting the high degree of predictive accuracy of the reported device; 95% of the validation data is found to lie within an error band of ±10% as highlighted by the green lines in Figure 4.

The analytical sensitivity of a sensor mainly concerns its limit of detection, i.e., the lowest concentration that can be distinguished as a signal after filtering out the background noise. The analytical sensitivity of a quantitative assay is usually determined using end-point dilution until the assay can no longer detect the target in more than 95% of the replicate cases. However, since our proposed technology is not a direct quantitative sensing platform but an implicit classification tool

https://doi.org/10.1021/acssensors.2c00806
ACS Sens. 2022, 7, 2028−2036

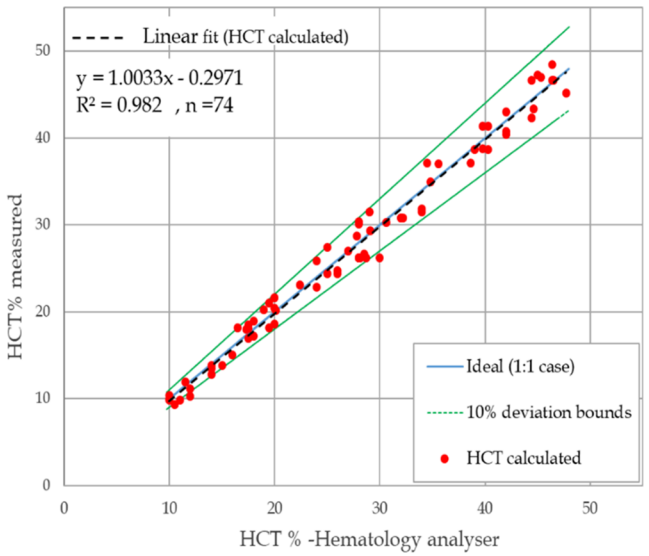

Figure 4. Comparison of the results from our HCT screening device with gold standard hematology analyzer for 74 whole blood samples. The blue line indicates the ideal case in which the device data coincide with the gold standard data. The black dashed line shows the best linear fit for the calculated HCT data. The green line represents the variation limits of ±10% from the gold standard data; 95% of the data is found to lie within this interval of ±10% error bands.

intended for clinical screening purposes, we rather focused on the clinical sensitivity (hereafter referred to as simply "sensitivity") and specificity of the sensor that reflects the direct efficacy of the resulting outcome for clinical decision-making purposes. Sensitivity indicates how likely a diagnostic test is to detect a condition when it is truly present in a patient, while specificity refers to the ability of a test to rule out the presence of a disease when it is actually not present in the patient.[44] Equations 3a and3b represent the standard protocols for calculating sensitivity and specificity values, respectively, where TP represents number of true positives, FP represents number of false positives, TN stands for number of true negatives, and FN stands for number of false negatives.

$$\text{sensitivity} = \text{TP} \div (\text{TP} + \text{FN}) \tag{3a}$$

$$\text{specificity} = \text{TN} \div (\text{TN} + \text{FP}) \tag{3b}$$

Out of the 74 validation samples, 56 were anemic (HCT < 37%); out of these, 27 samples belonged to the category of severe anemia (HCT < 21%) and the remaining 29 samples indicated moderate to high level of anemia. By setting the detection thresholds at HCT = 21% and HCT = 37% for extreme and moderate levels of anemia, respectively, our POC testing method yielded sensitivity and specificity values of 96.3 and 100%, respectively, for screening severe anemia, and 96.5 and 100%, respectively, while screening between moderate anemia and normal conditions. Out of the total number of validation samples, three samples belonging to borderline ranges of the classified groups were screened erroneously with false-negative results; one severely anemic sample was wrongly classified as moderately anemic and two moderately anemic samples were misjudged as healthy ones.

Cross-Reactivity Effects on the Detection Performance. Through experimental trials, we further verified the cross-reactivity effect of several non-HCT elements in the blood on the obtained fractal dimension of the fingering patterns to corroborate our findings. Keeping in the purview of the practical constraints with respect to the availability of blood samples having exactly the same HCT value albeit discernibly different values of other significant diagnostic parameters (such as cholesterol, globulins, platelets, glucose), we tried to collect blood samples with nearly similar HCT levels, yet reflecting the patient-specific variabilities in several such other reported parameters. To assess the effect of fibrinogen content of blood on the viscous fingering, we performed experiments with RBC suspensions of volume fraction 25% (in isotonic saline) spiked with different concentrations of standard fibrinogen (Sigma-Aldrich, India). With regard to the effect of fibrinogen concentration, we were compelled in resorting to the spiking approach since the same is not routinely available as common benchmarked diagnostic data reported from the pathology labs, unlike other common hematological parameters. In all of these scenarios, we found that regardless of the wide-scale variation of each of these parameters, the fractal dimension of the blood pattern remained almost unaffected for a particular value of the HCT%. The experimental data of the cross-reactivity tests are provided in Tables S5a−e. This observation, though appearing to be summarily phenomenological, may be rationalized from the following considerations: (i) the roles of these cross-influential pathological parameters toward altering the blood viscosity are deemed to be more prominent under bulk flow conditions as opposed to a short transient of the spreading regime, (ii) the spreading volume of blood here is only about 20 μL where the fractional occupation of RBC is significantly more decisive in altering the blood rheology compared to other elements present with relatively tracer concentration levels, and (iii) the quantitative parameter extracted here for the screening purposes is an index deciphering the self-similarity of the blood spreading topology as against any absolute measure of the blood viscosity itself so that perturbations due to the influences of other interfering factors render to be inconsequential for the targeted quantitative analytics of concern.

It is also important to mention here that while the present method was established to be highly sensitive and specific so far as the blood HCT level determination is concerned, there is no evidenced rationale of mapping the same with any particular diseased condition as a standalone feature. Several possible diseased (renal disease,[4] Vitamin-B12 deficiency,[3] chronic liver disease[45] and leukemia,[5] diabetes,[46] hypertension,[47] metabolic syndrome[48]) lifestyle and medication conditions may culminate to a common observable influence on the blood HCT level. Recognizing this aspect, we have not claimed the sensor platform developed here as a confirmatory diagnostic testing instrument. Rather, the utilitarian implication of the present technology may be best realized in a screening test format to identify vulnerable patients requiring emergent medical attention. Possible follow-up investigations may be performed for the identified vulnerable subjects toward arriving at closure to the clinical decision making, with the aid of additional clinical or complementary diagnostic evidences to feature disease-specific recommendations.

Effect of Background Illumination. A distinctive advantage offered by our screening device is that the test outcome is not affected by the variation in the ambient light intensity,[49] which eliminates the need for specialized illumination to be potentially coupled with the readout unit. All of the reported optical-signal-based assays for anemia screening, on the other hand, are sensitively dependent on the lighting conditions because of their precise quantitative

https://doi.org/10.1021/acssensors.2c00806
ACS Sens. 2022, 7, 2028−2036

mapping with the color-scale values or optical intensity parameters. The present method obviates this shortcoming by virtue of the fact that it correlates with the observed topology rather than the optical intensity. Figure S5 clearly establishes this proposition by evidencing the fact that although the respective grayscale intensities of the images obtained evidenced expected strong dependence on the background illumination, the HFD values of the corresponding blood patterns turned out to be insensitive to the background lighting conditions. This could enable a disruptive simplification of our sensor design by completely eliminating the need of additional instrumentation for illumination control.

Effect of On-Field Aberrations. Although the temperature of blood does affect its viscosity, our experiments revealed that the same does not turn out to be consequential with regard to the envisaged diagnostic outcome of concern here, particularly considering: (i) rapid timescale of the experimental observables (~35 s) and (ii) limited thermal variability under ambient conditions during each experimental run. To justify the proposition, we carried out experiments under three different ambient temperature conditions: (a) within air-conditioned laboratory at 18 °C, (b) within air-conditioned laboratory at 25 °C, and (c) in open-field settings at 37 °C. Samples of two different HCT values (42 and 30%) have been tested in the above three cases. For both the high and low HCT cases, it was found that the HFD values and the corresponding screening accuracy were completely unaffected by the change in ambient temperature. The experimental data are shown in Table S6. Physically, such concurrence may be attributed to the underlying geometric self-similarities in the observed topological patterns, which, for a given ambient temperature condition, are not likely to be influenced by the absolute temperature values during the experimental runs but more emphatically by the thermal fluctuations therein. Considering the ultrashort timescale of the experiments, these thermal fluctuations did not manifest discernible influences to alter the intrinsic topology of viscous fingering that solely governed our quantitative analytical outcome. In fact, in addition to the normal validation procedures, we also performed on-field testing with our device outside controlled laboratory settings for 25 patient samples, out of which 20 belonged to normal healthy category and 5 belonged to moderate to highly anemic regime. The results (as highlighted in Table S8) indicate excellent screening efficacy (100% screening accuracy) of our device even in extreme point-of-care conditions, as attributable to the following decisive advantageous features: (i) an approach that is completely devoid of specialized reagents and instrumentation, resolving the otherwise common bottlenecks of specialized lab access and supply chain of sensitive consumables in uncontrolled settings, and (ii) amenability of use by minimally trained frontline workers as against specialized lab technicians.

Cost Benefits. The sensor developed here is of ultralow cost that requires only one-time investment of a camera-integrated smartphone as the capital asset that has otherwise become a household commodity by virtue of unprecedented advances in consumer electronic gadgets, telecommunication, and mobile network outreach. The only recurring costs include those of standard filter paper and a tiny volume of glycerol per test. Given the availability of a standard smartphone, this implies that the test may be disseminated virtually for free, which offers an extremely favorable value proposition compared to other more elaborate POC-based anemia detection counterparts.[50] Table S7 enlists some of the key advantageous features of the present testing approach, as against some other POC-based methods for anemia detection used in current practice.

CONCLUSIONS

We demonstrated the use of a simple paper strip with no fabrication steps involved for rapid screening of anemia using static image analysis of the pattern formed by the spreading front of one drop of blood, without necessitating any sensitive reagents, by exploiting a physical phenomenon that appears to be omnipresent in engineering and living systems.[51−57] In contrast to the common chemically or electrochemically based principles of diagnostic testing with body fluids, the present method completely relies on an intriguing physics-based principle that finger-like projections at the interface may develop when a drop of blood spreads over a paper matrix pre-saturated with glycerol. We experimentally determined an interconnection between the observed morphological features of the interface and the blood HCT level and translated the same to a single quantified parameter, namely, the fractal dimension that has been demonstrated to be a highly accurate marker for rapid screening of potentially vulnerable anemic patients via trivial smartphone integration without any additional auxiliary hardware requirement, demanding no control in the background lighting for the image acquisition. The method has been established to be sufficiently repeatable and reproducible without compromising the accuracy of the test outcome, even in extreme resource-limited settings, and may constitute the basis of a new class of diagnostic testing procedure by harnessing the physics at fluidic interfaces.

ASSOCIATED CONTENT

Supporting Information

The Supporting Information is available free of charge at https://pubs.acs.org/doi/10.1021/acssensors.2c00806.

Effect of sample storage time on detection result; effect of the height of blood drop release on detection efficacy; determination of the order of magnitude of shear rate through paper; effect of porosity of the paper strip; flow diagram of the box-counting method; reproducibility analysis; cross-reactivity studies (effect of cholesterol, fibrinogen, globulin, platelets, and glucose) on the fractal dimension of blood pattern; effect of background illumination; tabular comparison of the present method with existing POC assays for anemia screening; and screening results for on-field testing (PDF)

AUTHOR INFORMATION

Corresponding Author

Suman Chakraborty − *Department of Mechanical Engineering, Indian Institute of Technology Kharagpur, Kharagpur 721302 West Bengal, India;* orcid.org/0000-0002-5454-9766; Email: suman@mech.iitkgp.ac.in

Authors

Sampad Laha − *Department of Mechanical Engineering, Indian Institute of Technology Kharagpur, Kharagpur 721302 West Bengal, India*

Aditya Bandopadhyay − *Department of Mechanical Engineering, Indian Institute of Technology Kharagpur,*

https://doi.org/10.1021/acssensors.2c00806
ACS Sens. 2022, 7, 2028−2036

Kharagpur 721302 West Bengal, India; orcid.org/0000-0003-3371-7879

Complete contact information is available at: https://pubs.acs.org/10.1021/acssensors.2c00806

Author Contributions

S.L. contributed to experimental work and reporting, graphical representation of results, and paper drafting. A.B. supported image analysis and manuscript proofreading. S.C. contributed to conceptualization of the entire work and problem definition, fund acquisition, supervision of the research, analysis and interpretation, paper drafting, and comprehensive editing.

Funding

This research work has been sponsored by Government funding (Ministry of Education and ICMR) through IMPRINT India scheme (Project Code: 4429), and the CRTDH scheme on "Affordable Healthcare" as sponsored by the Department of Scientific and Industrial Research, Government of India.

Notes

The authors declare no competing financial interest.

■ ACKNOWLEDGMENTS

The authors gratefully acknowledge the help of the members of the pathology section of B. C. Roy Technology Hospital of their parent institute for sample collections as per the guidelines prescribed by the Institutional Ethical Committee, as well as for providing gold standard hematology analysis data. S.C. acknowledges Department of Science and Technology, Government of India, for Sir J. C. Bose National Fellowship. The authors also thank Subhamoy Chatterjee of the Department of Electronics and Electrical Communication Engineering of the Institute for his valuable suggestions on the Android app development.

■ REFERENCES

(1) WHO Report. Iron Deficiency Anaemia: Assessment, Prevention, and Control; **2001**.
(2) Osazuwa, F.; Ayo, O. Contribution of Malnutrition and Malaria to Anemia in Children in Rural Communities of Edo State, Nigeria. *North Am. J. Med. Sci.* **2010**, 532−536.
(3) Yeruva, S. L. H.; Manchandani, R. P.; Oneal, P. Pernicious Anemia with Autoimmune Hemolytic Anemia: A Case Report and Literature Review. *Case Rep. Hematol.* **2016**, *2016*, No. 7231503.
(4) Babitt, J. L.; Lin, H. Y. Mechanisms of Anemia in CKD. *J. Am. Soc. Nephrol.* **2012**, *23*, 1631−1634.
(5) Troup, S. B.; Swisher, S. N.; Young, L. E. The Anemia of Leukemia. *Am. J. Med.* **1960**, *28*, 751−763.
(6) Kosiborod, M.; Smith, G. L.; Radford, M. J.; Foody, J. M.; Krumholz, H. M. The Prognostic Importance of Anemia in Patients with Heart Failure. *Am. J. Med.* **2003**, *114*, 112−119.
(7) Lichtman, M. A.; Beutler, E.; Selighson, U.; Kaushansky, K.; Kipps, T. O. *Williams Hematology*, 7th ed.; McGraw-Hill, 1995.
(8) Paradis, N. A.; Balter, S.; Davison, C. M.; Simon, G.; Rose, M. Hematocrit as a Predictor of Significant Injury after Penetrating Trauma. *Am. J. Emerg. Med.* **1997**, *15*, 224−228.
(9) Goldenfarb, P. B.; Bowyer, F. P.; Hall, E.; Brosious, E. Reproducibility in the Hematology Laboratory: The Microhematocrit Determination. *Am. J. Clin. Pathol.* **1971**, *56*, 35−39.
(10) Fleisher, M.; Gladstone, M.; Crystal, D.; Schwartz, M. K. Two Whole-Blood Multi-Analyte Analyzers Evaluated. *Clin. Chem.* **1989**, *35*, 1532−1535.
(11) Lee, H. Y.; Barber, C.; Rogers, J. A.; Minerick, A. R. Electrochemical Hematocrit Determination in a Direct Current Microfluidic Device. *Electrophoresis* **2015**, *36*, 978−985.
(12) Jalal, U. M.; Kim, S. C.; Shim, J. S. Histogram Analysis for Smartphone-Based Rapid Hematocrit Determination. *Biomed. Opt. Express* **2017**, *8*, 3317.
(13) Kang, Y. A Disposable Blood-on-a-Chip for Simultaneous Measurement of Multiple Biophysical Properties. *Micromachines* **2018**, *9*, 475.
(14) Chakraborty, S.; Das, S.; Das, C.; Chandra, S.; Sharma, K.; Das; Karmakar, A.; Chattoapadhyay, S. On-Chip Estimation of Hematocrit Level for Diagnosing Anemic Conditions by Impedimetric Techniques. *Biomed. Microdevices* **2020**, *22*, 38.
(15) Treo, E. F.; Felice, C. J.; Tirado, M. C.; Valentinuzzi, M. E.; Cervantes, D. O. Comparative Analysis of Hematocrit Measurements by Dielectric and Impedance Techniques. *IEEE Trans. Biomed. Eng.* **2005**, *52*, 549−552.
(16) Agarwal, R.; Sarkar, A.; Bhowmik, A.; Mukherjee, D.; Chakraborty, S. A Portable Spinning Disc for Complete Blood Count (CBC). *Biosens. Bioelectron.* **2020**, *150*, No. 111935.
(17) Riegger, L.; Grumann, M.; Steigert, J.; Lutz, S.; Steinert, C. P.; Mueller, C.; Viertel, J.; Prucker, O.; Rühe, J.; Zengerle, R.; Ducrée, J. Single-Step Centrifugal Hematocrit Determination on a 10-$ Processing Device. *Biomed. Microdevices* **2007**, *9*, 795−799.
(18) Gilmore, J.; Islam, M.; Martinez-Duarte, R. Challenges in the Use of Compact Disc-Based Centrifugal Microfluidics for Healthcare Diagnostics at the Extreme Point of Care. *Micromachines* **2016**, *7*, 52.
(19) Li, H.; Steckl, A. J. Paper Microfluidics for Point-of-Care Blood-Based Analysis and Diagnostics. *Anal. Chem.* **2019**, *91*, 352−371.
(20) Bialkower, M.; Manderson, C. A.; McLiesh, H.; Tabor, R. F.; Garnier, G. Paper Diagnostic for Direct Measurement of Fibrinogen Concentration in Whole Blood. *ACS Sens.* **2020**, *5*, 3627−3638.
(21) Komatsu, T.; Maeki, M.; Ishida, A.; Tani, H.; Tokeshi, M. Paper-Based Device for the Facile Colorimetric Determination of Lithium Ions in Human Whole Blood. *ACS Sens.* **2020**, *5*, 1287−1294.
(22) Guan, L.; Tian, J.; Cao, R.; Li, M.; Cai, Z.; Shen, W. Barcode-Like Paper Sensor for Smartphone Diagnostics: An Application of Blood Typing. *Anal. Chem.* **2014**, *86*, 11362−11367.
(23) Narayana Iyengar, S.; Dietvorst, J.; Ferrer-Vilanova, A.; Guirado, G.; Muñoz-Berbel, X.; Russom, A. Toward Rapid Detection of Viable Bacteria in Whole Blood for Early Sepsis Diagnostics and Susceptibility Testing. *ACS Sens.* **2021**, *6*, 3357−3366.
(24) Li, L.; Huang, X.; Liu, W.; Shen, W. Control Performance of Paper-Based Blood Analysis Devices through Paper Structure Design. *ACS Appl. Mater. Interfaces* **2014**, *6*, 21624−21631.
(25) Yamada, K.; Suzuki, K.; Citterio, D. Text-Displaying Colorimetric Paper-Based Analytical Device. *ACS Sens.* **2017**, *2*, 1247−1254.
(26) Khachornsakkul, K.; Dungchai, W. Rapid Distance-Based Cardiac Troponin Quantification Using Paper Analytical Devices for the Screening and the Follow-Up of Acute Myocardial Infarction, Using a Single Drop of Human Whole Blood. *ACS Sens.* **2021**, *6*, 1339−1347.
(27) Kar, S.; Maiti, T. K.; Chakraborty, S. Capillarity-Driven Blood Plasma Separation on Paper-Based Devices. *Analyst* **2015**, *140*, 6473−6476.
(28) Berry, S. B.; Fernandes, S. C.; Rajaratnam, A.; DeChiara, N. S.; Mace, C. R. Measurement of the Hematocrit Using Paper-Based Microfluidic Devices. *Lab Chip* **2016**, *16*, 3689−3694.
(29) McGann, P. T.; Tyburski, E. A.; de Oliveira, V.; Santos, B.; Ware, R. E.; Lam, W. A. An Accurate and Inexpensive Color-Based Assay for Detecting Severe Anemia in a Limited-Resource Setting. *Am. J. Hematol.* **2015**, *90*, 1122−1127.
(30) Tyburski, E. A.; Gillespie, S. E.; Stoy, W. A.; Mannino, R. G.; Weiss, A. J.; Siu, A. F.; Bulloch, R. H.; Thota, K.; Cardenas, A.; Session, W.; Khoury, H. J.; O'Connor, S.; Bunting, S. T.; Boudreaux, J.; Forest, C. R.; Gaddh, M.; Leong, T.; Lyon, L. A.; Lam, W. A.

Disposable Platform Provides Visual and Color-Based Point-of-Care Anemia Self-Testing. *J. Clin. Invest.* **2014**, *124*, 4387−4394.
(31) Biswas, S. K.; Chatterjee, S.; Bandyopadhyay, S.; Kar, S.; Som, N. K.; Saha, S.; Chakraborty, S. Smartphone-Enabled Paper-Based Hemoglobin Sensor for Extreme Point-of-Care Diagnostics. *ACS Sens.* **2021**, *6*, 1077−1085.
(32) Frantz, E.; Li, H.; Steckl, A. J. Quantitative Hematocrit Measurement of Whole Blood in a Point-of-Care Lateral Flow Device Using a Smartphone Flow Tracking App. *Biosens. Bioelectron.* **2020**, *163*, No. 112300.
(33) Nijjer, J. S.; Hewitt, D. R.; Neufeld, J. A. The Dynamics of Miscible Viscous Fingering from Onset to Shutdown. *J. Fluid Mech.* **2018**, *837*, 520−545.
(34) Saffman, P. G.; Taylor, G. The Penetration of a Fluid into a Porous Medium or Hele-Shaw Cell Containing a More Viscous Liquid. *Proc. R. Soc. Lond., Ser. A: Math. Phys. Sci.* **1958**, *245*, 312−329.
(35) Zimmerman, W. B.; Homsy, G. M. Viscous Fingering in Miscible Displacements: Unification of Effects of Viscosity Contrast, Anisotropic Dispersion, and Velocity Dependence of Dispersion on Nonlinear Finger Propagation. *Phys. Fluids* **1992**, *4*, 2348−2359.
(36) Tan, C. T.; Homsy, G. M. Simulation of Nonlinear Viscous Fingering in Miscible Displacement. *Phys. Fluids* **1988**, *31*, 1330.
(37) Antwi-Baffour, S. Prolong Storage of Blood in EDTA Has an Effect on the Morphology and Osmotic Fragility of Erythrocytes. *Int. J. Biomed. Sci. Eng.* **2013**, *1*, 20.
(38) Walburn, F. J.; Schneck, D. J. A Constitutive Equation for Whole Human Blood. *Biorheology* **1976**, *13*, 201−210.
(39) Kar, S.; Dash, M.; Maiti, T. K.; Chakraborty, S. Effect of Hematocrit on Blood Dynamics on a Compact Disc Platform. *Analyst* **2015**, *140*, 1432−1437.
(40) Otsu, N. Threshold selection method from gray-level histograms. *IEEE Trans. Syst. Man Cybern.* **1979**, *9*, 62−66.
(41) Schwarzenberger, R.; Falconer, K. Fractal Geometry: Mathematical Foundations and Applications. *Math. Gaz.* **1990**, *74*, 316.
(42) Ostwald, M. J.; Vaughan, J. *The Fractal Dimension of Architecture*; Springer International Publishing: Cham, 2016.
(43) "Red Cell Transfusion Guidelines", Washington State Clinical Laboratory Advisory Council, 2009 https://www.doh.wa.gov/Portals/1/Documents/2700/RedCell.pdf (accessed: 4 February 2020).
(44) Maxim, L. D.; Niebo, R.; Utell, M. J. Screening Tests: A Review with Examples. *Inhalation Toxicol.* **2014**, *26*, 811−828.
(45) Gonzalez-Casas, R.; Jones, E. A.; Moreno-Otero, R. Spectrum of Anemia Associated with Chronic Liver Disease. *World J. Gastroenterol.* **2009**, *15*, 4653.
(46) Soliman, A. T.; De Sanctis, V.; Yassin, M.; Soliman, N. Iron Deficiency Anemia and Glucose Metabolism. *Acta Biomed.* **2017**, *88*, 112−118.
(47) Atsma, F.; Veldhuizen, I.; de Kort, W.; van Kraaij, M.; Pasker-de Jong, P.; Deinum, J. Hemoglobin Level Is Positively Associated With Blood Pressure in a Large Cohort of Healthy Individuals. *Hypertension* **2012**, *60*, 936−941.
(48) Timerga, A.; Haile, K.; Dessu, S. Anemia and Associated Factors among Patients Admitted with Metabolic Syndromes at Worabe Comprehensive Specialized Hospital, Southern Ethiopia: A Cross-Sectional Study. *PLoS One* **2022**, *17*, No. e0266089.
(49) Yang, X.; Piety, N. Z.; Vignes, S. M.; Benton, M. S.; Kanter, J.; Shevkoplyas, S. S. Simple Paper-Based Test for Measuring Blood Hemoglobin Concentration in Resource-Limited Settings. *Clin. Chem.* **2013**, *59*, 1506−1513.
(50) Rippmann, C. E.; Nett, P. C.; Popovic, D.; Seifert, B.; Pasch, T.; Spahn, D. Hemocue, an Accurate Bedside Method of Hemoglobin Measurement? *J. Clin. Monit.* **1997**, *13*, 373−377.
(51) Bandopadhyay, A.; Mandal, S.; Kishore, N. K.; Chakraborty, S. Uniform electric-field-induced lateral migration of a sedimenting drop. *J. Fluid Mech.* **2016**, *792*, 553−589.
(52) Kar, S.; Maiti, T. K.; Chakraborty, S. Capillarity-driven blood plasma separation on paper-based devices. *Analyst* **2015**, *140*, 6473−6476.
(53) Raj, P. M.; Sarkar, S.; Chakraborty, S.; Phanikumar, G.; Dutta, P.; Chattopadhyay, K. Modelling of transport phenomena in laser surface alloying with distributed species mass source. *Int. J. Heat Fluid Flow* **2002**, *23*, 298−307.
(54) Goswami, P.; Chakraborty, S. Semi-analytical solutions for electroosmotic flows with interfacial slip in microchannels of complex cross-sectional shapes. *Microfluid. Nanofluid.* **2011**, *11*, 255−267.
(55) Chakraborty, S. Order parameter modeling of fluid dynamics in narrow confinements subjected to hydrophobic interactions. *Phys. Rev. Lett.* **2007**, *99*, No. 094504.
(56) Kunti, G.; Bhattacharya, A.; Chakraborty, S. Rapid mixing with high-throughput in a semi-active semi-passive micromixer. *Electrophoresis* **2017**, *38*, 1310−1317.
(57) Talapatra, S.; Chakraborty, S. Double layer overlap in ac electroosmosis. *Eur. J. Mech. B* **2008**, *27*, 297−308.

Recommended by ACS

Smartphone-Enabled Paper-Based Hemoglobin Sensor for Extreme Point-of-Care Diagnostics
Sujay K. Biswas, Suman Chakraborty, *et al.*
FEBRUARY 26, 2021
ACS SENSORS
READ

Current and Emerging Microfluidic-Based Integrated Solutions for Free Hemoglobin and Hemolysis Detection and Measurement
Noman Naeem, Maïwenn Kersaudy-Kerhoas, *et al.*
DECEMBER 03, 2021
ANALYTICAL CHEMISTRY
READ

Point-of-Care Assessment of Hemostasis with a Love-Mode Surface Acoustic Wave Sensor
Xi Chen, Gang Zhao, *et al.*
JANUARY 06, 2020
ACS SENSORS
READ

The "Bloodless" Blood Test: Intradermal Prick Nanoelectronics for the Blood Extraction-Free Multiplex Detection of Protein Biomarkers
Nimrod Harpak, Fernando Patolsky, *et al.*
AUGUST 25, 2022
ACS NANO
READ

Get More Suggestions >

https://doi.org/10.1021/acssensors.2c00806
ACS Sens. 2022, 7, 2028−2036